NGR-05-002-294

CALIFORNIA INSTITUTE OF TECHNOLOGY

BIG BEAR SOLAR OBSERVATORY

HALE OBSERVATORIES

[redacted]

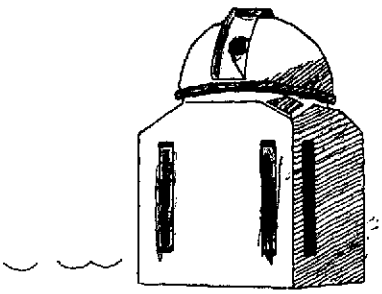

SLOW X-RAY BURSTS AND CHROMOSPHERIC FLARES WITH FILAMENT DISRUPTION

by

J.-René Roy and Frances Tang

BIG BEAR SOLAR OBSERVATORY, HALE OBSERVATORIES

CARNEGIE INSTITUTION OF WASHINGTON

CALIFORNIA INSTITUTE OF TECHNOLOGY

Pasadena, California, U.S.A.

BBSO #0141

ABSTRACT

The data from OGO-5 and OSO-7 X-ray experiments have been analyzed to study six chromospheric flares with filament disruption associated with slow thermal X-ray bursts. Filament activation accompanied by a slight X-ray enhancement precedes the first evidence of Hα flare by a few minutes. Rapid increase of the soft X-ray flux is accompanied by a sudden brightening of the filament when viewed on-band Hα. Thereafter the bright chromospheric strands reach their maximum brightness with maximum X-ray flux. Any plateau or slow decay phase in the X-ray flux is accompanied by a quieting in filament activity and even by filament re-appearance. The height of the disrupted prominence is proportional to the soft X-ray flux for the August 3, 1970 limb occulted event. Analysis of the X-ray bursts on 2220 UT June 23, 1972 gives a 'cool' maximum temperature of 12.5×10^6 K and a maximum emission measure of 40×10^{47} cm^{-3}.

Conduction is shown to be a more efficient cooling mechanism of the hot flare plasma than radiation. Initial heating probably occurs in the vicinity of the filament and filament activation may visualize some magnetic field changes which heat up the X-ray emitting plasma.

1. INTRODUCTION

Conventionally, solar X-ray bursts contain emission of two general types. In the range below 10 keV, thermal emission from a plasma assumed to have a Maxwellian electron distribution with temperatures ranging between 1.0 - 2.0 x 10^7 K dominates the spectrum (Culhane and Phillips, 1969; Datlowe et al., 1974a). At higher energy, the spectrum is represented as a power law of the form $F(h\nu) = A(h\nu)^{-\gamma}$ where $F(h\nu)$ is the flux in photons $cm^{-2}s^{-1}keV^{-1}$ and γ the spectral index. It is still being questioned whether this spectrum arises from a distribution of very high temperature ($\approx 10^8$K) plasmas (Chubb, 1970; Brown, 1973) or from the non-thermal bremsstrahlung of accelerated electrons (Holt and Ramaty, 1969; Brown, 1971).

Most recent studies on solar X-ray bursts have concentrated on powerful impulsive thermal events of which 2/3 have correlated non-thermal events (Datlowe et al., 1974 b). X-ray emission which behaves slowly with time in the form of powerful long duration thermal events has been known to be related to type IV radio bursts and post-flare loop prominence systems (Datlowe et al., 1974a). Thomas and Teske (1971) and Drake (1971) have demonstrated the dependence of the soft X-ray flux on the time history of the Hα flare area and brilliance.

In the present work, we draw attention to a category of soft thermal bursts associated with chromospheric Hα flares

accompanied by dark filament disruption. Because the disrupted filament evolves in the corona above the chromospheric flare, any relationship between the evolution of the filament and the X-ray emission could lead to some clues on flare heating.

2. INSTRUMENTATION

The Hα observations were obtained at the Big Bear Solar Observatory. Two 10-inch refractors produced large-scale cinematographic data at Hα up to $\pm$ 1 Å. Observations of the full disk in Hα were made with an 8.6-inch vacuum refractor. The X-ray data are from OGO-5 Berkeley and OSO-7 UCSD X-ray experiments. Details on both experiments can be found respectively in Kane and Anderson (1970) and Harrington et al., (1973). The OGO-5 experiment used a scintillator with eight logarithmically-spaced channels between 9.6 and > 128 keV; the saturation level in each individual channel is about 2.8×10^4 counts s^{-1}. Due to pulse pile-up (Kane and Hudson, 1970), OGO-5 data do not offer as good a separation of the hard X-ray component from the low energy thermal component as the more recent OSO-7 experiment which used a two detector system: (i) a proportional counter with eight channels between 1-15 keV and (ii) a scintillator with nine logarithmically spaced channels between 10-370 keV.

The saturation level of the 5.1-6.6 keV channel is 3×10^4 photons $cm^{-2}s^{-1}keV^{-1}$.

3. OBSERVATIONAL DATA

Table I summarizes the observing parameters of the events; Figure 1 displays the accompanying X-ray bursts. These bursts accompany Hα chromospheric flares occurring at the outskirt of active regions where the average magnetic field is about 100 gauss; the flares are of the two-ribbon type similar to those described by Kiepenheuer (1963), Smith and Ramsey (1964), Hyder (1967) and Dodson and Hedeman (1970). The filament disruptions are of the "quasi-eruptive" type described by Martin (1973) where the prominence ascends but flows back to the chromosphere in its later stage. The X-ray bursts accompanying these flares have durations >1 hour, characterized by a slow rise and decay time (20-40 min); large flux fluctuations over periods of 5-10 min are common. The absence of a definite impulsive non-thermal component in the >10 keV X-ray flux is puzzling because of the occurrence of short impulsive spikes in the microwave flux for the September 27, 1970 event (Figure 2b). Weak peaks were present in the OSO-7 20-30 keV channel for a very short interval associated with a sharp increase in the soft X-ray flux in the 2220 UT June 23, 1972 event. Sequences of activity at Hα are shown for the September 27, 1970 event on the disk and for the August 3, 1970 event over the limb in Figures 2a and 3a.

We summarize in Table II the most characteristic features of Hα emission and filament activation related to the thermal X-ray flux behavior for the six events of Table I. The numerals in Figure 1 refer to the successive phase numbers described in Table II. We define "slow" changes at Hα as changes that cannot be told apart from successive frames, i.e. about 15 sec, and "rapid" when definite changes are obvious between frames. The observation of these phases is not new: Smith and Ramsey (1964) give an identical time history for similar Hα events and refer to earlier works which recognized such patterns in Hα flares with filament disruption.

We find from the flares of Table I that changes in the filament appearance taking place in less than a few minutes rarely correlate with soft X-ray flux fluctuations; instead the filament major stages of development (activation and disruption) are always associated with well-defined phases in the soft X-ray emission. Referring to Table II we stress the stages of the filament evolution as related to definite intervals of the X-ray history.

Phase 1 acts like a precursor where soft X-ray emission accompanies filament activation prior to chromospheric Hα enhancement (Figure 1). However, filament activation in itself is not sufficient; we have a case of violent filament activation which is succeeded by neither

filament disruption nor flare, showing no X-ray flux enhancement on April 2, 1971 (1700 UT). Phase 2 is characterized by very little change in the X-ray flux and the initiation of the filament ascending motion which become more rapid in Phase 3. During Phase 4A, the rapid soft X-ray flux increase is first accompanied by the sudden brightening of the un-twisting filament; the filament brightens as if it was catching fire (Figure 4). The intense brightening of the Hα strands, taking the shape of the classical two-ribbon flare follows within minutes (Phase 4B). Phase 4A is visible in the flares happening near the limb and over the limb on October 10, 1971 and August 3, 1970. The intense chromospheric strands reach their maximum brightness with the X-ray flux (Phase 5).

If the soft X-ray flux reaches a plateau or starts decaying slowly (Phase 6A and 6B), there is an obvious quieting of filament motion; viewed at the limb, the erupted prominence slows down its expansion and takes a loop-shaped configuration (Figures 3a and 6). Gaps now develop near the top of the prominence and material flows down; the prominence general brightness fluctuates while the soft X-ray flux stays about the same or decays slowly. Figure 3b displays a striking relationship between the height of the disrupted filament above the limb and the 9.6-19.2 keV X-ray flux of the accompanying burst; the more filament one sees, the larger the X-ray flux that is recorded. In the September 27, 1970 event the X-ray flux

develops a saddle-shaped minimum point lasting about 10 min between two maxima. During this saddle phase, the filament is seen to reappear almost in its original configuration and with a similar contrast. As soon as the X-ray flux increases to the next maximum, the filament slowly disappears again (Figure 2a).

4. ANALYSIS OF THE 2220 UT JUNE 23, 1972 X-RAY BURST

We have analyzed the 2220 UT June 23, 1972 X-ray event in McMath 11930 for its physical parameters. The event is typical of those listed in Table I and sufficient X-ray data are available to give insight into the evolution of the associated X-ray flare. The maximum flux in the 5.1-6.6 keV channel is about 2×10^3 photons $cm^{-2}s^{-1}keV^{-1}$. Little flux is measured in the 20-30 keV channel; only two tiny spikes reaching the level of 0.1 photons $cm^{-2}s^{-1}keV^{-1}$ are seen in this channel at 2220 and 2221 UT (Figure 5). These two spikes coincide with the sudden increase in the soft X-ray channel and also with a violent phase in the disruption of the filament. Meanwhile a simple 3 microwave burst was recorded at 2700 MHz from Pentincton starting at 2210 UT.

The temperature of the X-ray emitting plasma can be calculated by taking the ratio of the fluxes measured in the different energy intervals (Datlowe et al., 1974a). Knowing the flux at the satellite and the temperature of the

plasma allows the calculation of the emission measure N_e^2V. As shown in Figure 5b the thermal burst in McMath 11930 behaves normally: a maximum temperature of 1.25×10^7K is reached at 2220 UT and the temperature decreases thereafter. The emission measure increases slowly to a maximum of about 4×10^{48} cm^{-3} at 2224:30 UT. Datlowe et al. (1974a) have found that the median maximum temperature of 197 X-ray bursts they analyzed was 1.6×10^7K. The maximum temperature of the X-ray burst associated with the filament disruption actually falls at the low end of this distribution and therefore it is a cool flare.

Culhane et al. (1970) have investigated in detail the cooling of flare plasma by electron Coulomb collisions, radiation and conduction. They show that conduction is probably the main cooling mechanism because of its dominating importance at high temperature. Conduction cooling places less stringent requirements on the density and volume of the flare plasma than do other processes. One may roughly estimate the volume of the flare plasma by using the area covered by the chromospheric emission as seen at Hα (450 arc sec^2 for the flare in McMath 11930) times the height of the corona involved in the burst. We assume the height to be at most of the order of the mean between the width and the length of the flare, i.e. about 40 arc sec. The estimated coronal volume is then approximately 8×10^{27}cm^3. We know from the analysis of the X-ray burst that the emission measure

$N_e^2 V = 4 \times 10^{48} cm^{-3}$; this leads to a density $N_e \simeq 3 \times 10^{10} cm^{-3}$. A larger volume would lower this density and vice-versa.

One may define a characteristic cooling time τ such that

$$(\tau)^{-1} = \frac{1}{T}\frac{dT}{dt} \simeq \frac{1}{T_a}\frac{\Delta T}{\Delta t} \qquad (1)$$

where ΔT is the change in the computed temperature over the time interval Δt as given by the X-ray spectrum analysis and T_a is the average temperature over the same interval.

The time scale for radiative cooling is expressed in a convenient form by

$$t_R = \frac{3\ kT}{N_e\ L_R} \qquad (2)$$

For the burst under consideration $T \simeq 10^7 K$. The plasma cooling rate coefficient L_R at this temperature is $10^{-23} ergs\ cm^{+3} sec^{-1}$ (Culhane et al., 1970). This gives approximately $t_R = 2 \times 10^4 sec$, which is much longer than the cooling time $\tau \simeq 800$ sec obtained from the temperature history of the event. In order to make $t_R = \tau$, we need to multiply the above N_e estimate by 25; accordingly, the value of the emission measure would then require a flare volume 600 times smaller than we estimated, which we believe to be unrealistic. For conduction cooling, the lack of electron mobility across the magnetic field lines converts the problem to one dimension. The relevant length is the dimension ℓ along the magnetic

field lines threading the flare. In such a configuration, the time scale for loss by conduction is given by

$$t_C = \frac{3\, N_e k\, \ell^2}{\kappa} \tag{3}$$

where

$$\kappa = 1.844 \times 10^{-5} \frac{T^{5/2}}{\ln\Lambda} \text{ ergs sec}^{-1}\text{cm}^{-1}\text{k}^{-1} \tag{4}$$

and is the coefficient of thermal conductivity parallel to the magnetic field for fully ionized hydrogen (Spitzer, 1962). Delcroix and Lemaire (1969) showed that κ changes only slightly by including the effect of a variety of abundance ratios of He and heavier elements. For the temperature and density ranges considered $\ln\Lambda \approx 20$ (Spitzer, 1962). With $T \approx 10^7$K, the coefficients of thermal conductivity is 3.16×10^{11} ergs sec^{-1} $\text{cm}^{-1}\text{k}^{-1}$. The dependence for the conduction cooling time scale on ℓ^2 makes it very sensitive to the characteristic length chosen. Flare ribbons occur at the feet of loop-shaped magnetic field lines connecting opposite polarities (Roy, 1972 and Rust and Bar, 1973). Cooling takes place along field lines; therefore, it is reasonable to assume that the distance separating the Hα ribbons is a good estimate of that scale; $\ell \approx 1.2 \times 10^9$cm. Using 3×10^{10} cm^{-3} for the density gives $t_C = 60$ sec. Even increasing ℓ by an order of magnitude would still keep the time

for conduction cooling short enough to make conduction effective. To have $t_c = \tau$, we need $\ell \simeq 4.4 \times 10^9$ cm.

If the observed compactness of the Hα flare justifies a small value for ℓ, the release of energy has to proceed throughout the burst lifetime since cooling by conduction is so rapid. Because conduction cooling is rapid, a lower temperature X-ray emitting plasma than typical probably arises from a slower than normal energy input rate. Moreover, the irregularities of the observed 5.1-6.6 keV X-ray flux in Figure 5a indicate fluctuations in the energy release.

5. INTERPRETATION

We have related phases of the filament activation and evolution with characteristic stages of the X-ray flux time profile, e.g. phases 1, 2, 3, 4A, 6A and 6B of Table II. We now discuss the possible physical relationships between these two aspects of solar flares. It is unlikely that X-rays originate from the filament itself because of its low temperature ($\simeq 10^4$K). Instead, X-ray emission probably arises from the hot coronal surrounding where the acting energy release mechanism also leads to the filament disruption. The similarity in the evolution of the X-ray flux and the height of the Aug. 3, 1970 disrupted filament where the lower levels are occulted by the limb also suggests that both phonomena have a same physical origin, possibly the rearranging coronal magnetic field. Instances of

filament activation occurring prior to strong Hα chromospheric enhancement (Phases 1, 2 and 4A) suggest that flare heating may first occur in the vicinity of the filament.

The sudden brightening of the filament in phase 4A can be interpreted as (i) Hα Doppler brightening or (ii) change in the physical conditions of the filament:

(i) If scattering dominates the Hα line source function of active region filaments, radial motion with respect to the sun could give rise to Doppler brightening whose amount depends on velocity, height and geometry of the moving material (Rompolt, 1967 and Hyder and Lites, 1970). The change in intensity is due to the Doppler-shifted chromospheric radiation field "seen" by the moving prominence; the effect is purely of geometrical and kinematic nature. Phase 4A is observed simultaneously to violent untwisting motions of the filament which may provide sufficient Doppler-shift to account for the sudden "flaming" of the filament. However, it is not known whether active region filaments are optically thin enough for their source function to be dominated by scattering; otherwise they would need to be sufficiently filamentary in structure that the chromospheric radiation field is able to penetrate them entirely. A sudden brightening of an active region filament was observed at HeI 10830 Å by David M. Rust (1974, unpublished) with the Sacramento Peak diode array during the 1547 UT April 13, 1974 flare. Outside plages HeI 10830 Å has no

significant chromospheric line; this weakens the Doppler brightening for HeI 10830 Å and suggests that Doppler brightening might not be a sufficient explanation.
(ii) The brightening could also be explained by a sudden change of the physical conditions inside the filament. Because phase 4A coincides with the rising X-ray flux, it is conceivable that the hot coronal surroundings at 10^7 K may transfer heat to the imbedded filament material and modify the parameters N_e and T_e.

The time lapse of a few minutes between the filament brightening and the appearance of strong chromospheric enhancement is of the same order as the conduction cooling time derived in section four. With phase 4B, the conduction path may be to the transition region and to the chromosphere which acts as better energy sinks through radiation. The quieting of the filament motion accompanying plateaux or saddle-shaped minimum points in the X-ray flux time profile presumably reflects diminished magnetic field reconnection -- if this is the flare heating mechanism.

We have chosen the slow X-ray bursts because they allow us to compare more easily the evolution of the filament with the X-ray emission. However, flares with filament disruption can associate with powerful soft and hard X-ray bursts as well, such as the Oct. 10, 1971 event (Figures 1 and 6). These impulsive bursts basically differ

from the former ones by their power, i.e. the amount of energy released per unit of time. This difference may arise from the higher strength of the surrounding magnetic field which would determine the magnitude of the energy release and the occurrence of non-thermal processes.

6. SUMMARY

We have studied flares with filament disruption at the boundaries of active regions corresponding to areas of medium magnetic field strength; these events are associated with slow X-ray bursts emitting mostly thermal radiation.

(1) Filament activation accompanied by a slight X-ray enhancement precedes the first evidence of Hα flare by 5 - 10 minutes.

(2) Rapid increase of X-ray flux is first accompanied by sudden brightening of the filament itself when viewed at Hα $\pm$ 0 Å .

(3) The bright chromospheric strands which appeared during (2) now reach their maximum brightness with the maximum X-ray flux.

(4) Any plateau or slow decay phase in the soft X-ray flux accompanies a slowing down of filament motion and even filament reappearance.

We conclude that filament activation may visualize some of the changes in the strength and configuration of the magnetic field which heat up the X-ray emitting coronal plasma.

ACKNOWLEDGEMENTS

We are grateful to Hugh S. Hudson and Dayton W. Datlowe of the University of California, San Diego, to Ronald L. Moore, Sou-Yang Liu and Harold Zirin of the California Institute of Technology, and to David M. Rust of Sacramento Peak Observatory for their helpful discussions and comments. The X-ray data was kindly provided by D. W. Datlowe (OSO-7) and S. Kane (OGO-5).

We acknowledge support from U.S. Air Force contract F19628-73-C-0085 and NASA Grant NGR 05-002-294.

REFERENCES

Brown, J. C.: 1971, Solar Phys. 18, 489.

Brown, J. C.: 1973, in G. Newkirk (Ed.) "Coronal Disturbances" IAU Symp. #57

Chubb, T. A.: 1970, in Dyer (Ed.) "Solar Terrestrial Physics I 1970" D. Reidel Pub. Co. Part I, 99.

Culhane, J. L. and Philips, K. J. H.: 1969, Solar Phys. 11, 117.

Culhane, J. L., Vesceky, J. F. and Philips, K. J. H.: 1970, Solar Phys. 15, 394.

Datlowe, D. W., Hudson, H. S. and Peterson, L. E.: 1974a, Solar Phys. in press.

Datlowe, D. W., Elcan, M. and Hudson, H. S.: 1974b, submitted to Solar Phys.

Delcroix, A. and Lemaire A.: 1969, Astrophys. J. 156, 787

Dodson, H. W. and Hedeman, E. R.: 1970, Solar Phys. 13, 401.

Drake, J. F.: 1971, Solar Phys. 16, 152.

Harrington, T. M., Maloy, J. O., McKenzie, D. L. and Peterson, L. E.: 1972 IEEE Trans. Nuc. Sci. NS-19, 596.

Holt, S. S. and Ramaty, R.: 1969, Solar Phys. 8, 119.

Hyder, C. L.: 1967, Solar Phys. 2, 267.

Hyder, C. L. and Lites, B. W.: 1970, Solar Phys. 14, 147.

Kane, S. R. and Anderson, K. A.: 1970, Astrophys. J. 162, 1003.

Kane, S. R. and Hudson, H. S.: 1970, Solar Phys. 14, 414.

Kiepenheuer, K. O.: 1963, in AAS-NASA Symposium on the Physics of Solar Flares, 323

Martin, S.: 1973, Solar Phys. 31, 3.

McKenzie, D. L., Datlowe, D. W. and Peterson, L. E.: 1973, Solar Phys. 28, 173.

Rompolt, B.: 1967, Acta Astron. 17, 329.

Roy, J.-R.: 1972, Solar Phys. 26, 418.

Rust, D. M. and Bar, V. J.: 1973, Solar Phys. 33, 445.

Smith, S. F. and Ramsey, H. E.: 1964, Z. Astrophys. 60, 1.

Spitzer, L.: 1972, Physics of Fully Ionized Gases, Interscience, 170 p.

Thomas, R. J. and Teske, R. G.: 1971, Solar Phys. 16, 431.

Table I

Chromospheric flares with filament disruption

Date	Time (UT)	McMath Region	Position	Importance	Maximum X-ray flux
Aug. 3, 70	1633	10846	N17 W90	Eruptive prom.	2×10^3*
Sept. 27, 70	i) 2139	10959	N16 W20	2N	8×10^3*
	ii) 2212	10959	N15 W18	1F	7×10^3*
Oct. 14, 70	2043	10979	N17 W33	-F	0.5×10^3*
Oct. 11, 71	0042	11537	N12 W73	1N	$>79.0 \times 10^3$**
May 5, 72	i) 2202	11856	S22 E42	--F	0.08×10^3**
	ii) 2232	11856	S18 E42	-N	1.1×10^3**
June 23, 72	2222	11930	S11 W26	-B	2.0×10^3**

* OGO-5 (9.6-19.2 keV channel) counts sec^{-1}

** OSO-7 (5.1-6.6 keV channel) photons $cm^{-2}s^{-1}keV^{-1}$

Table II

Development of X-ray bursts associated with flares with filament disruption

Phase	X-ray emission	Duration	Hα activity
1	Increase of soft X-ray flux a few times above background.	5-10 min	Filament activation: changes in contrast; no Hα chromospheric emission.
2	Slight decrease of soft X-ray flux.	5-10 min	slow rising of filament.
3	Continuation of phase 2.	10-15 min	Filament rapid expansion; some Hα chromospheric
4A	Rapid rise of X-ray flux to maximum; possible microwave and hard X-ray bursts.	10-15 min	Hα sudden brightening of twisting filament; filament disruption at Hα off-band.
4B			Appearance of bright Hα strands.
5	Maximum soft X-ray flux.	2-5 min	Maximum chromospheric brightness at Hα.
6A	Plateau or very slow decay of soft X-ray flux.	10 min	Termination of filament motion or gaps formation in eruptive prominence on limb.
6B	Formation of a saddle-shaped minimum point in X-ray flux.		Filament reappearance.
7	Slow decay of soft X-ray flux.	60 min	Decay of Hα brightness; change in former filament location and/or appearance of dark lane.

FIGURE CAPTIONS

Figure 1. X-ray counting rates as function of time and energy for the bursts accompanying the flares with filament disruption. The various numerals along the curves refer to phases described in table II. (University of California, San Diego and Berkeley)

Figure 2a. Time history of the chromospheric flare viewed at H$\alpha \pm 0$ Å on Sept. 27,1970. The event is accompanied by a filament disruption. The reappearance of the filament at 2150:36 UT corresponds to the saddle-shaped minimum point in the X-ray flux in figure 1. (Big Bear Solar Observatory).

Figure 2b. 2700 MHz microwave flux of the Sept. 27, 1970 event. The partially occulted event of Aug. 3, 1970 produced no microwave enhancement. (Dominion Radio Astro. Physical Observatory, Pentincton)

Figure 3a. Time history of a disrupting filament originating beyond the west limb on Aug. 3, 1970. The interest of this event lies in the fact that the corresponding chromospheric Hα flare is occulted by the limb. The associated X-ray burst is shown in Figure 1. The microwave flux at 10 cm shows no enhancement. We identify the filament on the filtergram taken the day before (Aug. 2). The peak X-ray flux around

1642 UT (Figure 1) is due to a surge event occurring in the same active center near the end of the filament disruption.

Figure 3b. X-ray flux and height of the disrupted filament of the Aug. 3, 1970 limb event versus time.

Figure 4. 'Before-and-during' Hα filtergrams showing phases 4A of the whole filament sudden brightening simultaneously to violent untwisting motion. This phase occurs during rising X-ray flux. (Big Bear Solar Observatory)

Figure 5. (a) X-ray burst accompanying the flare of 2220 UT June 23, 1972. The satellite went into eclipse at time of maximum X-ray flux.

(b) Temperature and emission measure derived from the analysis of the proportional counter rates for the June 23, 1972 event. (University of California, San Diego)

Figure 6. Time history of Hα ± 0 Å filtergrams of an event with filament disruption near the west limb. Compare with the Aug. 3, 1970 event in Figure 3. The accompanying X-ray burst is shown in Figure 1. (Big Bear Solar Observatory)

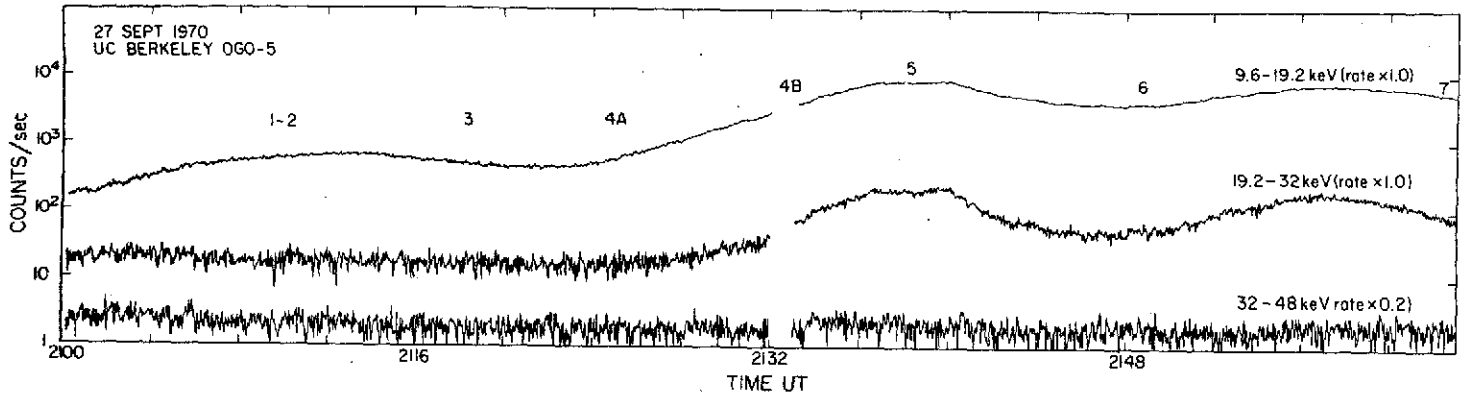
27 SEPT 1970
UC BERKELEY OGO-5
COUNTS/sec
1-2
3
4A
4B
5
6
7
9.6-19.2 keV (rate x1.0)
19.2-32 keV (rate x1.0)
32-48 keV rate x0.2)
2100
2116
2132
2148
TIME UT

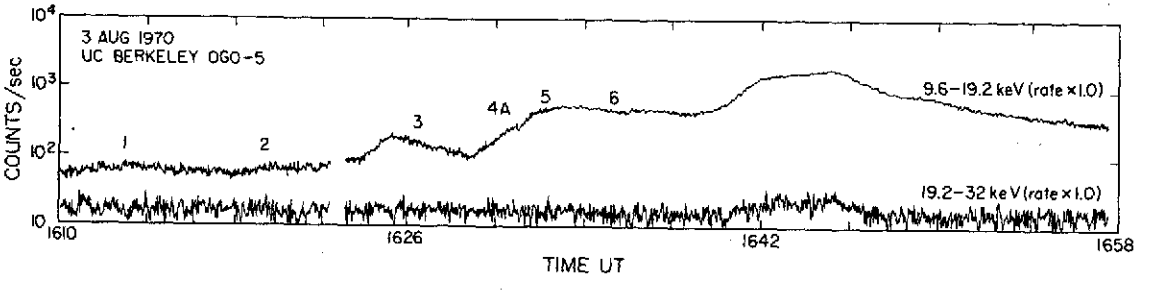
3 AUG 1970
UC BERKELEY OGO-5
COUNTS/sec
1
2
3
4A
5
6
9.6-19.2 keV (rate x1.0)
19.2-32 keV (rate x1.0)
1610
1626
1642
1658
TIME UT

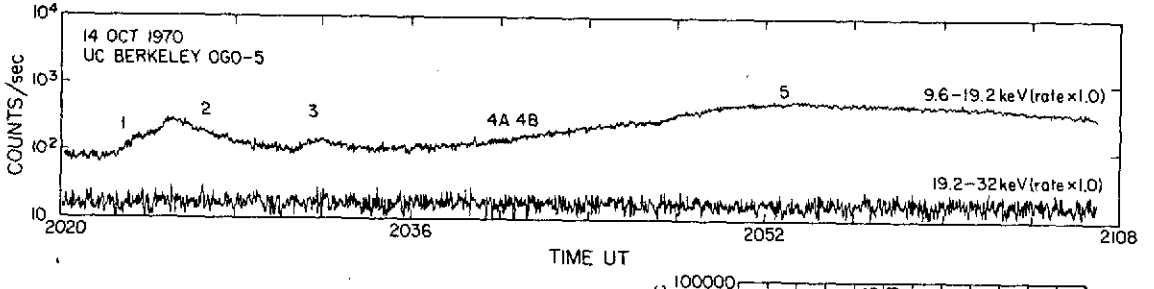
14 OCT 1970
UC BERKELEY OGO-5
COUNTS/sec
1
2
3
4A 4B
5
9.6-19.2 keV (rate x1.0)
19.2-32 keV (rate x1.0)
2020
2036
2052
2108
TIME UT

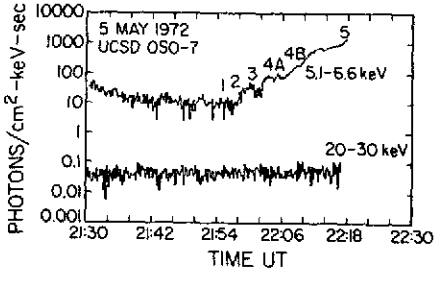
5 MAY 1972
UCSD OSO-7
PHOTONS/cm²-keV-sec
1
2
3
4A
4B
5
5.1-6.6 keV
20-30 keV
21:30
21:42
21:54
22:06
22:18
22:30
TIME UT

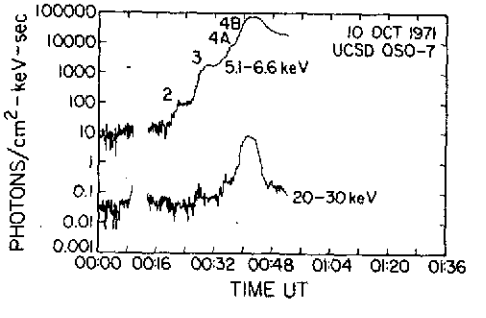
10 OCT 1971
UCSD OSO-7
PHOTONS/cm²-keV-sec
2
3
4A
4B
5.1-6.6 keV
20-30 keV
00:00
00:16
00:32
00:48
01:04
01:20
01:36
TIME UT

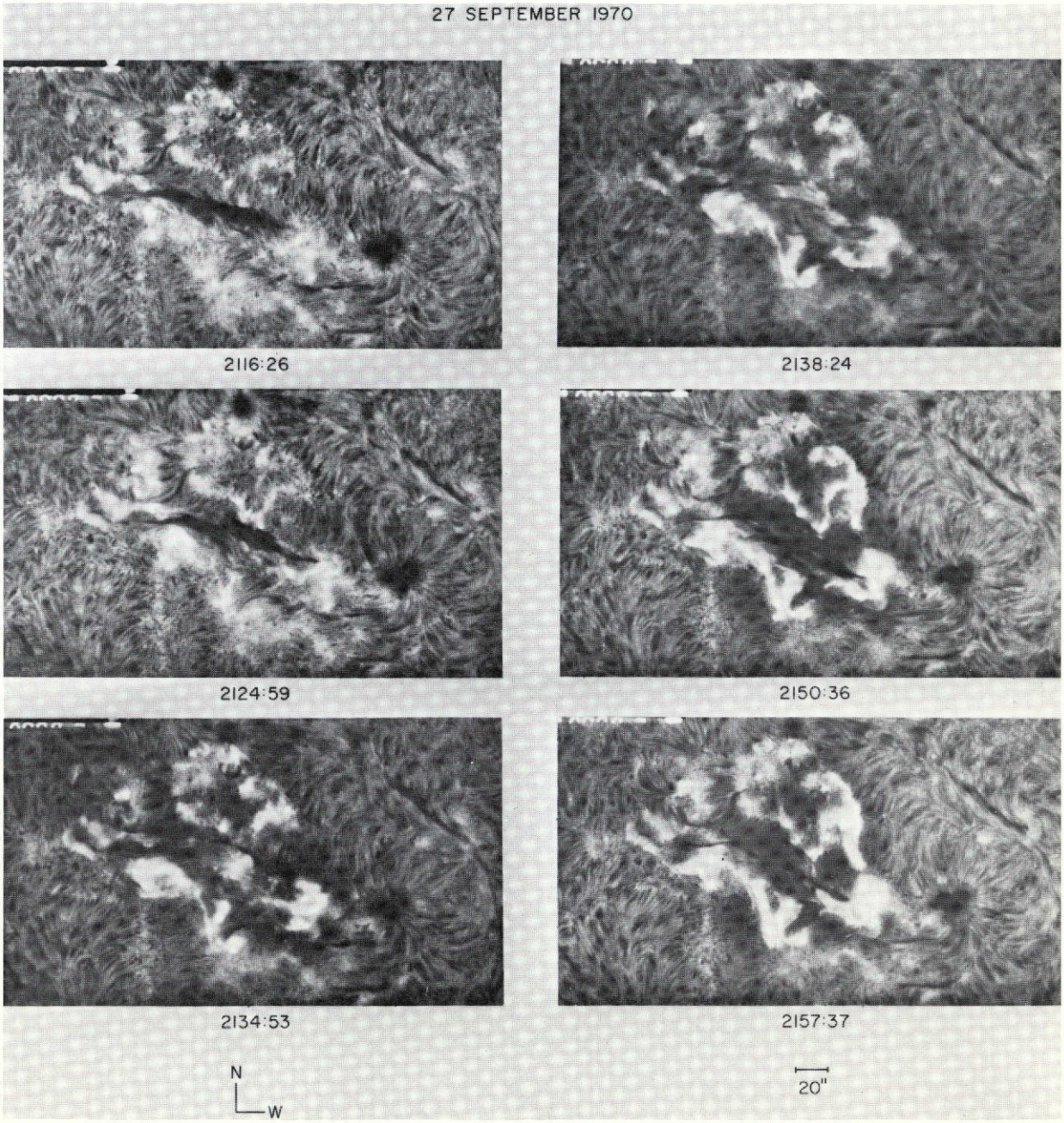
27 SEPTEMBER 1970
2116:26
2138:24
2124:59
2150:36
2134:53
2157:37
N
W
20"

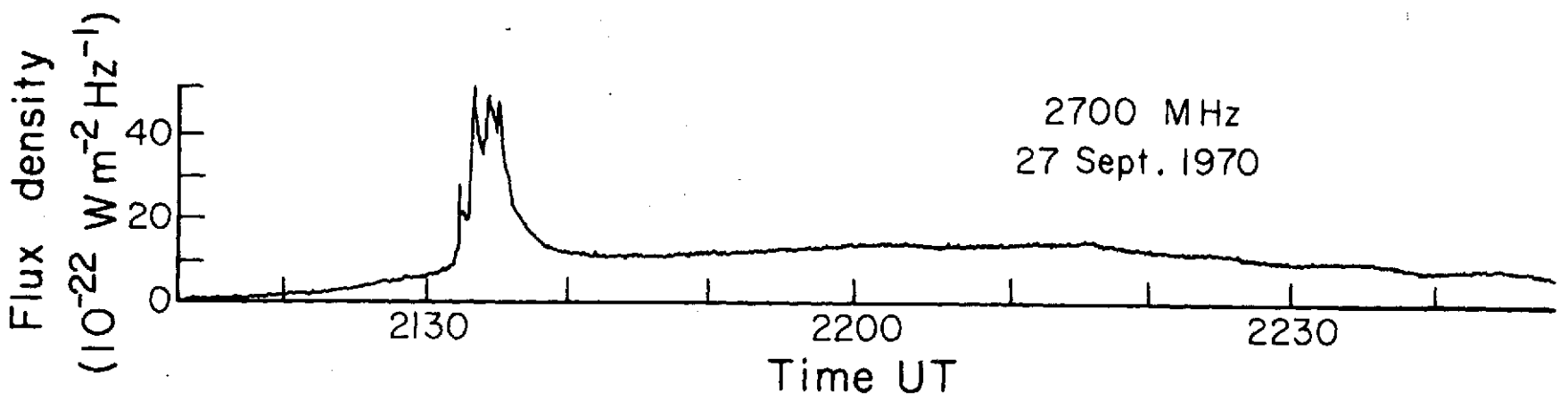
Flux density
(10^{-22} W m^{-2} Hz^{-1})
40
20
0
2130
2200
2230
Time UT
2700 MHz
27 Sept. 1970

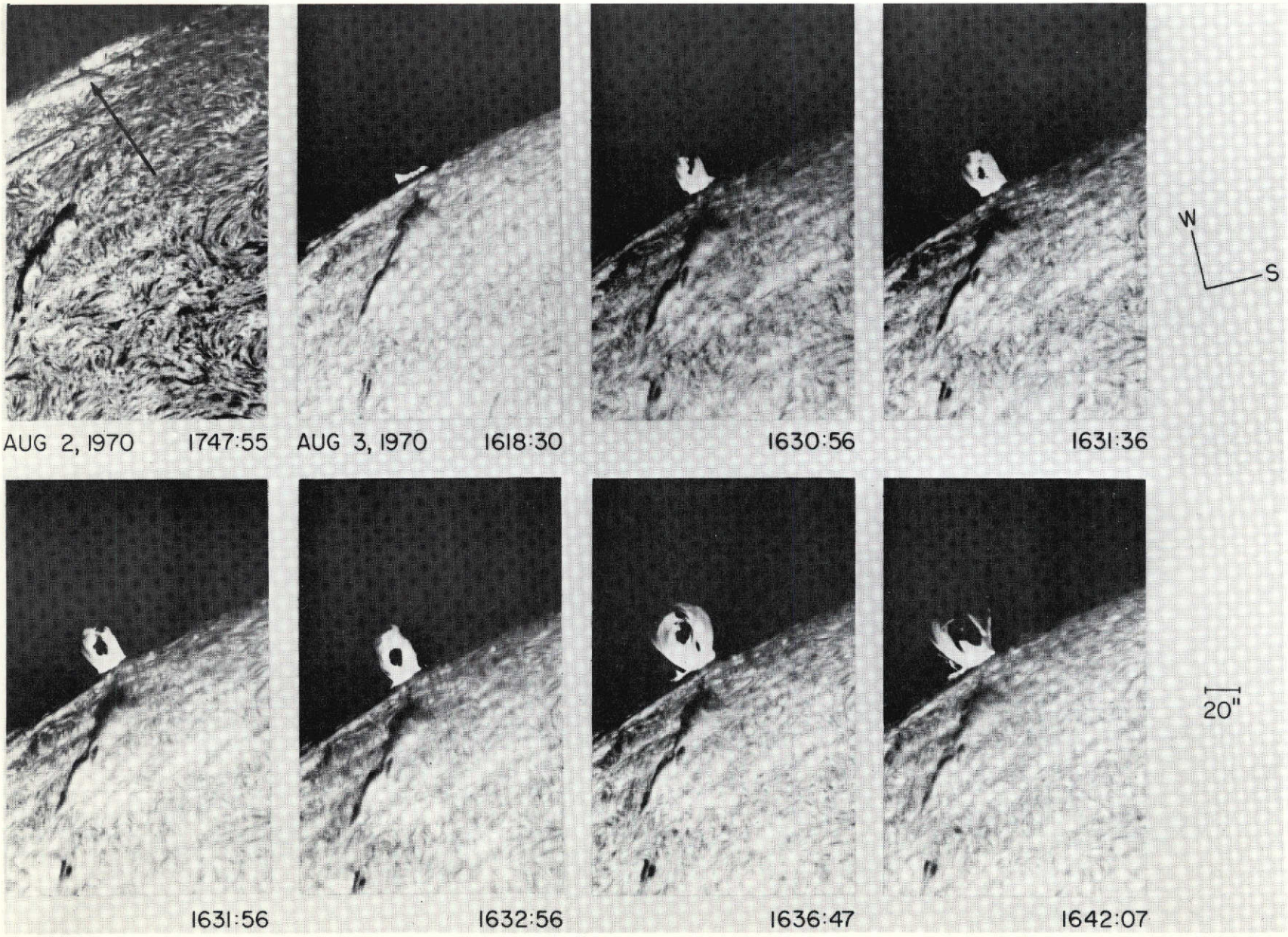
AUG 2, 1970 1747:55
AUG 3, 1970 1618:30
1630:56
1631:36
W
S
1631:56
1632:56
1636:47
1642:07
20"

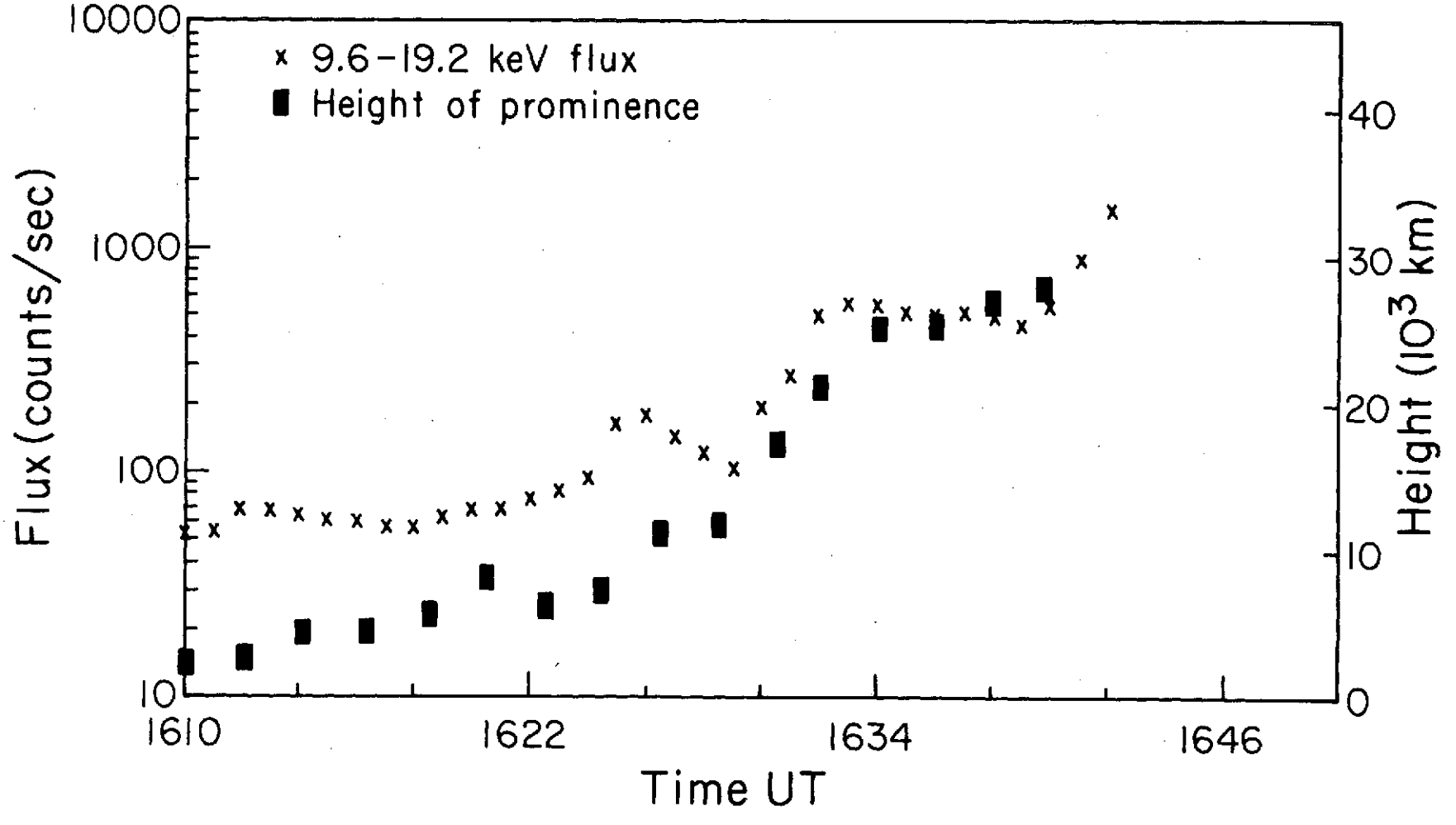
10000
1000
100
10
Flux (counts/sec)
x 9.6–19.2 keV flux
Height of prominence
40
30
20
10
0
Height (10^3 km)
1610
1622
1634
1646
Time UT

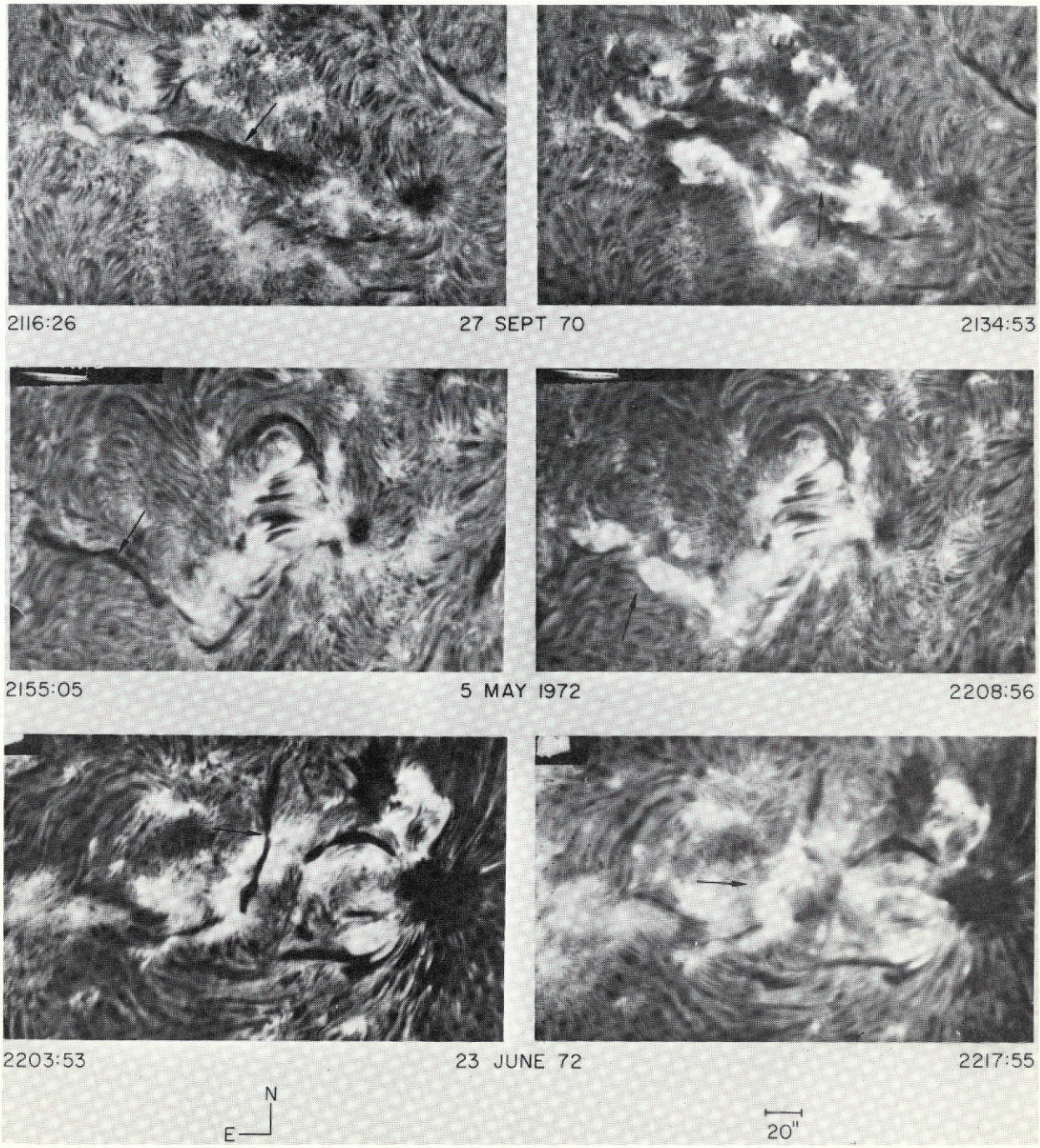
2116:26
27 SEPT 70
2134:53
2155:05
5 MAY 1972
2208:56
2203:53
23 JUNE 72
2217:55
N
E
20"

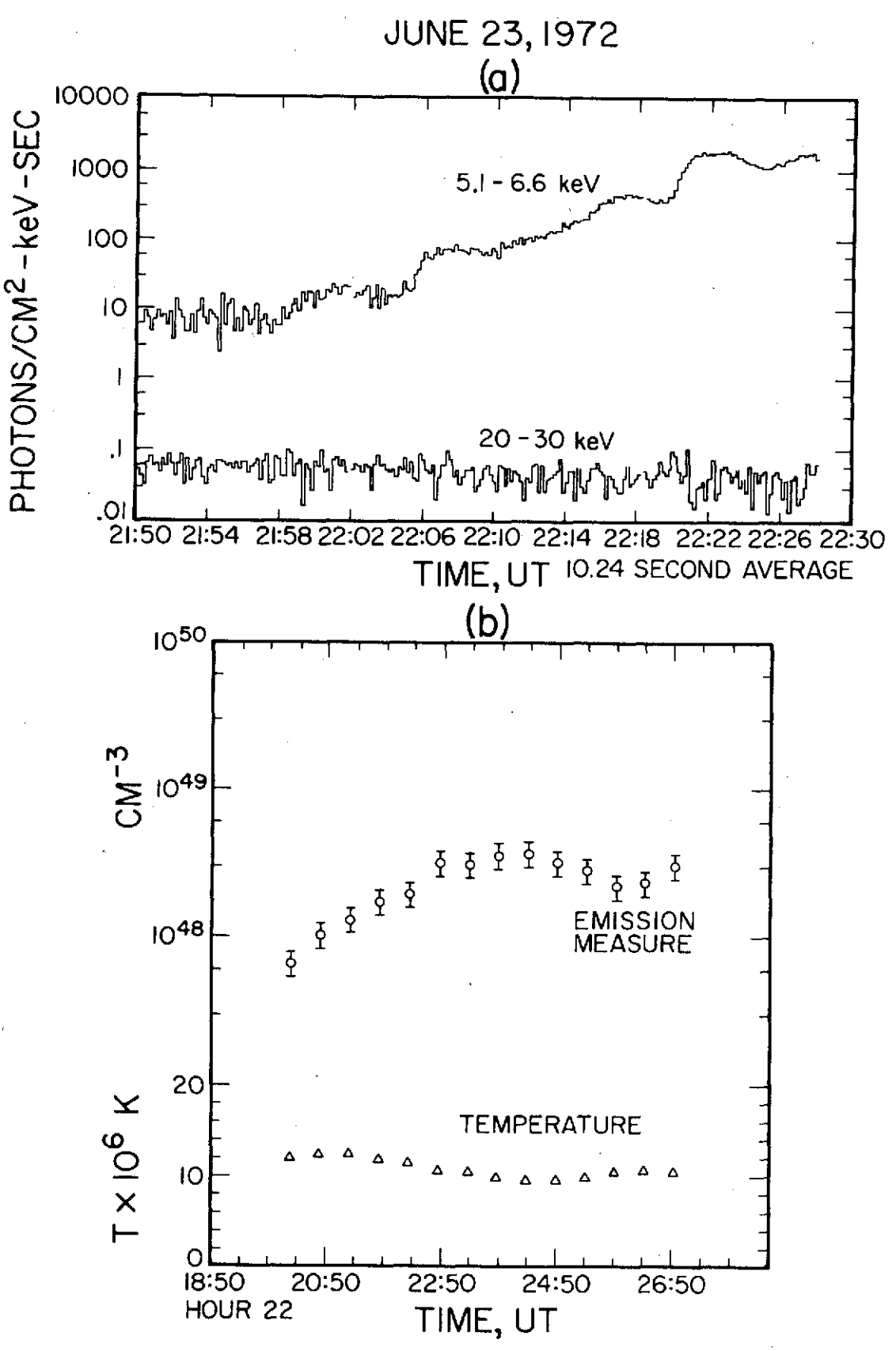

UCSD OSO-7 SOLAR X-RAY EXPERIMENT

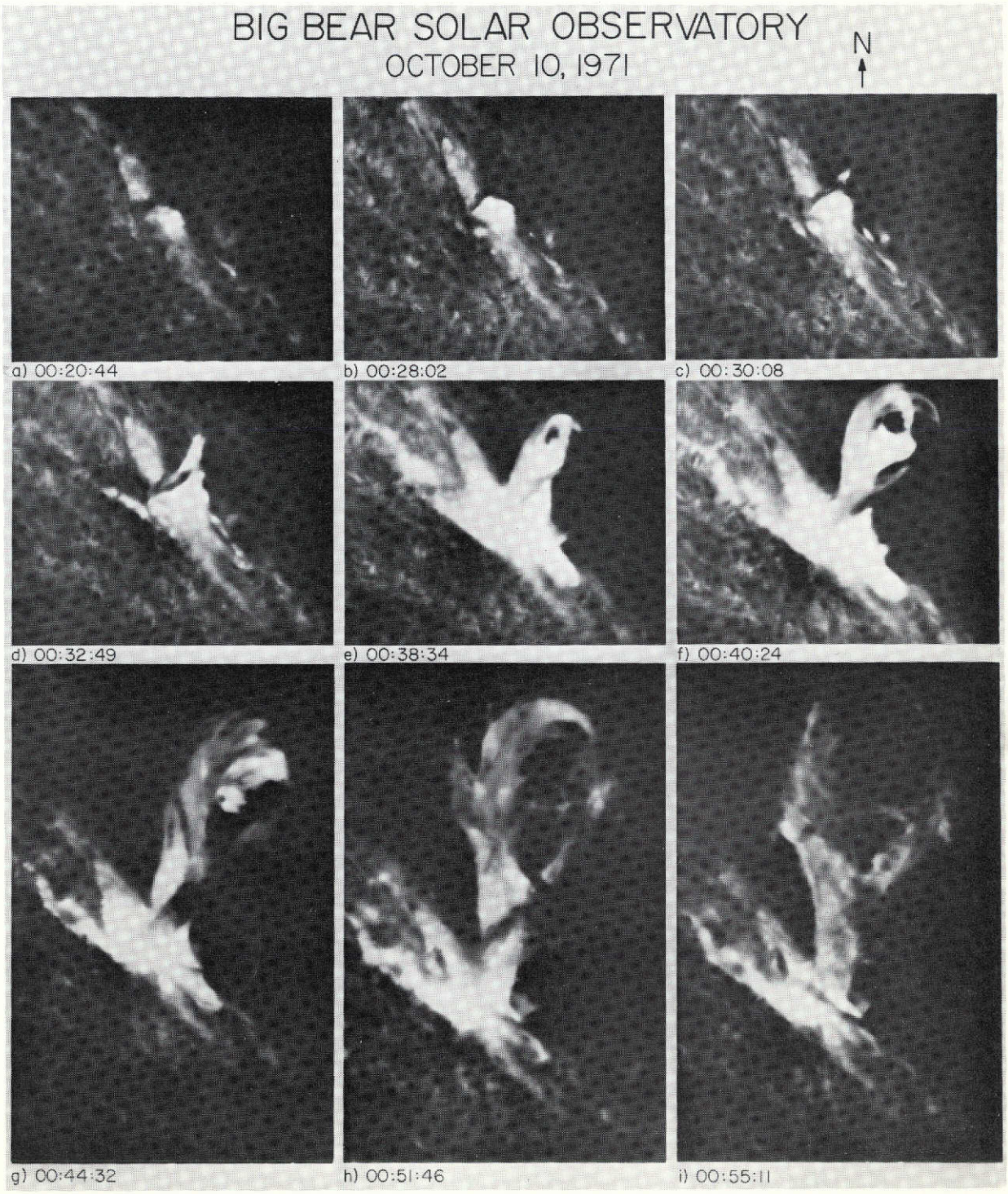
BIG BEAR SOLAR OBSERVATORY
OCTOBER 10, 1971
N
a) 00:20:44
b) 00:28:02
c) 00:30:08
d) 00:32:49
e) 00:38:34
f) 00:40:24
g) 00:44:32
h) 00:51:46
i) 00:55:11